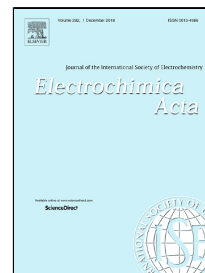


# Accepted Manuscript

Direct Measurement of Lithium Ion Fluxes with a Rotating Ring Disc Electrode in Potentiometric Mode

María del Pozo, Florencia Marchini, Leonardo Cantoni, Ernesto J. Calvo



PII: S0013-4686(18)32541-6  
DOI: 10.1016/j.electacta.2018.11.069  
Reference: EA 33070  
To appear in: *Electrochimica Acta*  
Received Date: 29 July 2018  
Accepted Date: 11 November 2018

Please cite this article as: María del Pozo, Florencia Marchini, Leonardo Cantoni, Ernesto J. Calvo, Direct Measurement of Lithium Ion Fluxes with a Rotating Ring Disc Electrode in Potentiometric Mode, *Electrochimica Acta* (2018), doi: 10.1016/j.electacta.2018.11.069

This is a PDF file of an unedited manuscript that has been accepted for publication. As a service to our customers we are providing this early version of the manuscript. The manuscript will undergo copyediting, typesetting, and review of the resulting proof before it is published in its final form. Please note that during the production process errors may be discovered which could affect the content, and all legal disclaimers that apply to the journal pertain.

# Direct Measurement of Lithium Ion Fluxes with a Rotating Ring Disc Electrode in Potentiometric Mode

María del Pozo†, Florencia Marchini, Leonardo Cantoni, Ernesto J. Calvo\*

INQUIMAE. Facultad de Ciencias Exactas y Naturales, Universidad de Buenos Aires.

Pabellón 2, Ciudad Universitaria. AR-1428 Buenos Aires. Argentina

## ABSTRACT:

Using potentiometric detection of lithium ions with a rotating ring disc electrode (RRDE), we report for the first time the simultaneous direct measurement of lithium ion fluxes for two experiments: a)  $O_2$  reduction in  $LiPF_6$  DMSO electrolyte and b) insertion and release of  $Li^+$  into and from  $LiMn_2O_4$  spinel structure in contact with aqueous  $Li^+$  ion solution. The theory of potentiometric RRDE developed for local pH measurement (Albery, Calvo, 1983) could be applied to obtain quantitative description of lithium surface concentration which differs from the analytical concentration under current flow. The new potentiometric technique can detect mismatch of electron and lithium ion fluxes.

Key words: lithium, RRDE, potentiometric,  $LiMn_2O_4$ , ORR

## Corresponding Author

\* Ernesto Julio Calvo. [calvo@qi.fcen.uba.ar](mailto:calvo@qi.fcen.uba.ar)

## Present Addresses

† María del Pozo, Departamento de Química Analítica y Análisis Instrumental, Universidad Autónoma de Madrid.

## INTRODUCTION

The theory of the potentiometric measurement with a ring electrode of a rotating ring disc electrode system (RRDE) has been developed by Albery and Calvo in 1983 for the measurement of surface pH changes.[1] This has been further developed by Albery and Mount [2, 3], and extended to the potentiometric measurement of the counter ion bromide.[4]

For a Faradaic process at the disc electrode, the theory provides a method to measure the surface concentrations at the ring electrode by a Nernstian potentiometric response and relates that concentration to the surface concentration at the disc electrode only by a geometric "detection efficiency" without disturbing the concentration profile. For complex multistep reactions, one can separate the contributions from different processes when the ion flux at the disc and the ring do not match according to the theory.

During the  $O_2$  reduction at Au disc electrode in lithium containing non aqueous electrolyte, a similar flux of  $Li^+$  towards the disc electrode should correspond to the  $O_2$  convective-diffusion flux. Therefore if the measured surface concentration of  $Li^+$ , detected by following the ring potential, is different from the bulk concentration a net lithium ion flux towards the electrode should match the incoming flux of oxygen.

Another interesting application of this potentiometric method to assess the surface concentration of ions is the intercalation process, for instance the intercalation/deintercalation reactions taking place at the surface of  $LiMn_2O_4$  in contact with lithium ion electrolyte. This is the case of lithium ion batteries in non aqueous solvents. We have also recently described a highly selective  $LiMn_2O_4$  - polypyrrole electrochemical cell for the extraction of  $LiCl$  from natural brine [5, 6]. Reproducible intercalation of  $Li^+$  in  $Li_xMn_2O_4$  ( $0 \leq x \leq 1$ ) and  $Cl^-$  in oxidized polypyrrole ( $PPy^+$ ) is achieved with an overall cell voltage of less 1V.  $LiMn_2O_4$  is a stable phase with half lithium content in the discharge curve

from  $\lambda$ - $\text{MnO}_2$  to  $\text{Li}_2\text{Mn}_2\text{O}_4$  [7, 8]. The mixed oxide  $\text{LiMn}_2\text{O}_4$  has a spinel structure (space-group  $\text{Fd}\bar{3}\text{m}$ ) and the unit cell contains 56 atoms: A cubic close-packed array of oxygen ions occupying the 32e sites; 16 Mn ions are located in the octahedral 16d sites ( $\text{MnO}_6$ ) and 8 Li ions in the tetrahedral 8a sites.[9] Lithium ions can be inserted in  $\lambda$ - $\text{MnO}_2$  cubic phase and extracted from  $\text{LiMn}_2\text{O}_4$  in aqueous solutions by a topotactic  $\text{Li}^+$  insertion reaction within the cubic symmetry with isotropic expansion of the cell.[10, 11] Recently, a mercury-capped platinum ultramicroelectrode (Hg/Pt UMEs) has been reported as amperometric probe for lithium ion concentration measurements using scanning electrochemical microscopy (SECM) [12, 13]. The potentiometric RRDE method, however, shows advantages over SECM approach since the forced convection eliminates the very serious concerns about thermally induced convective flows in the latter system.[14]

In this communication, we describe the theory and experiment to detect the surface lithium ion concentration using a potentiometric rotating ring disc electrode and the measurement of ion fluxes.

### Theory

We measure the electrode potential of an Au ring covered with  $\text{Li}_{1.5}\text{Mn}_2\text{O}_4$  with respect to a reference electrode with potential independent of lithium ion activity. For a net flux of  $\text{Li}^+$  ions incoming or outgoing from the disc electrode surface, the disc surface and hence the ring surface concentration differ from the bulk concentration.

For this we make use of the “detection efficiency” as compared to the “collection efficiency”.[15] The latter is a ratio of the ring to disc currents, while the former is the ratio of the concentration measured by the potentiometric ring electrode (zero flux on the ring) to the concentration at the disc surface:

$$N_d = \frac{\tilde{c}}{c_{D,0}} \quad (1)$$

Where  $c_{D,0}$  is the concentration at the disc surface, and  $\tilde{c}$  is the concentration at a point on the ring surface so that a zero net flux at the ring is set.

$$\int_{r_2}^{r_3} 2\pi(c - \tilde{c})dr = 0 \quad (2)$$

Both the collection and the detection efficiency are geometric parameters, i.e. they only depend on the ring-disc radii,  $r_1$ ,  $r_2$  and  $r_3$  and not on the electrochemical reaction. The surface concentration on the ring is proportional to the disc surface concentration and the proportionality constant, the potentiometric ‘‘Detection Efficiency Coefficient’’,  $N_D$ , only depends on the RRDE geometry:[1]

$$[Li^+]_{surf} = [Li^+]_{bulk} + \frac{N_D Z_{D,1}}{D_{Li}} \frac{|i_D|}{nF\pi r_1^2} W^{-1/2} \quad (3)$$

Where  $D_{Li}$  is the diffusion coefficient of lithium ions in the liquid electrolyte,  $r_1$  is the disc radius and  $W$  the rotation frequency in Hz,  $i_D$  is the disc current,  $\nu$  is the kinematic viscosity of the liquid, and  $Z_{D,1} = 0.64 \nu^{1/6} D_{Li}^{1/3}$  is the diffusion layer thickness for  $W = 1$  Hz.

The flux of lithium ions at the disc surface is given by:

$$j_{Li} = \frac{i_{Li}}{nF} = \frac{D_{Li} ([Li]_{surf} - [Li]_{bulk})}{N_D Z_{D,1} W^{-1/2}} = \frac{|I_D|}{nF\pi r_1^2} \quad (4)$$

If  $[Li^+]_{surf} \neq [Li^+]_{bulk}$   $j_{Li} \neq 0$  and  $i_D \neq 0$

$$j_{Li} = \frac{i_{Li}}{nF} = \frac{([Li]_{surf} - [Li]_{bulk})}{0.64 N_D \nu^{1/6} D_{Li}^{-2/3} W^{-1/2}} \quad (5)$$

Replacing  $Z_{D,1}$  in eqn. (3) and replacing in eqn. (5) we obtain the lithium ion current density, which can be compared to the total electron current at the disk for more complex situations:

$$i_{Li} = \frac{nF ([Li]_{surf} - [Li]_{bulk})}{0.64 N_D v^{1/6} D_{Li}^{-2/3} W^{-1/2}} \quad (6)$$

## EXPERIMENTAL PROCEDURES

All reagents were analytical grade and used without further purification. All solutions were prepared using ultrapure Milli-Q water (18M $\Omega$ ). Non-aqueous solution were prepared in anhydrous dimethyl sulfoxide (DMSO) inside the M-Braun glove box.

All electrochemical measurements were performed using an Autolab PGSTAT204 in a three electrode configuration, using the substrate as a working electrode, an Ag/AgCl (3 M KCl) or Li<sub>2</sub>Mn<sub>2</sub>O<sub>4</sub> / LiMn<sub>2</sub>O<sub>4</sub> (1M LiPF<sub>6</sub> in DMSO) as reference electrode and a large area polypyrrole counter electrode.

We have used a Au-Au rotating ring disc electrode system with the following geometry, Au disc  $r_1 = 0.25$  with 0.2 cm<sup>2</sup> area, inner and outer ring radius  $r_2 = 0.26$  cm,  $r_3 = 0.30$  cm respectively. The system has a detection coefficient  $N_D = 0.49$  in potentiometry mode calculated with the theory published elsewhere [1], while the amperometric mode collection efficiency is  $N_0 = -0.28$ . [16]

The Au disc electrode was covered by LiMn<sub>2</sub>O<sub>4</sub> with an ink prepared by mixing LiMn<sub>2</sub>O<sub>4</sub>, polyvinylidene fluoride (Sigma Aldrich) and Vulcan-XC72<sup>®</sup> carbon black (Cabot Corp.) in a mass ratio 8:1:1 respectively, and suspended in N-methyl pyrrolidone ( $\geq 99\%$ , Sigma-Aldrich). The LMO ink was prepared by mixing LiMn<sub>2</sub>O<sub>4</sub>, PVDF and carbon Vulcan<sup>®</sup> in a mass ratio 8 : 1 : 1 respectively, and suspended in NMP.

The ring electrode was covered with an ink prepared with Li<sub>2</sub>Mn<sub>2</sub>O<sub>4</sub>/LiMn<sub>2</sub>O<sub>4</sub>, which was synthesized by mixing LiMn<sub>2</sub>O<sub>4</sub> and LiI in a 2:1 molar ratio and heating at 100 °C under rough vacuum for 36 hours, with periodical grinding. The resulting equimolar mixture of Li<sub>2</sub>Mn<sub>2</sub>O<sub>4</sub> / LiMn<sub>2</sub>O<sub>4</sub> was then added to PVDF and carbon Vulcan<sup>®</sup> in a 8 : 1 : 1 mass

ratio, respectively. The mixture was finally suspended in NMP and stirred overnight to form the ink.

The amount of lithium manganese oxides deposited can be estimated in  $10\text{-}15\ \mu\text{g}\cdot\text{cm}^{-2}$  from a similar deposition of the slurry onto a Au coated quartz crystal microbalance.

The ring electrode  $\text{LiMn}_2\text{O}_4/\text{Li}_2\text{Mn}_2\text{O}_4$  with two oxide phases in contact with lithium ions in the electrolyte has only one degree of freedom, the lithium concentration in the electrolyte. The system has been used as a reference electrode in non aqueous electrolytes [17]. The electrode potential with respect to a lithium independent reference electrode is a measure of the lithium ion activity in the electrolyte. After preparation the electrode was equilibrated with a 0.1 M solution of lithium ions for 24 hours before use.

Since the electrode potential reflects the activity of lithium ions in the electrolyte, a calibration curve was determined for each electrolyte.

In the absence of changes in lithium concentration the Au ring electrode covered by  $\text{LiMn}_2\text{O}_4/\text{Li}_2\text{Mn}_2\text{O}_4$  shows a stable electrode potential. When the Au ring electrode was covered with the composite  $\text{LiMn}_2\text{O}_4/\text{Li}_2\text{Mn}_2\text{O}_4$  /carbon and equilibrated with LiCl solution, fast changes of the electrode potential operate upon changes in the lithium ion activity with a rise time less than 5 seconds.

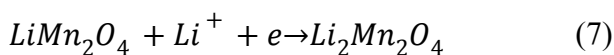
The ring electrode was connected to a high impedance ( $> 10^{12}\ \Omega$ ) differential voltage follower based on IC LMC6064 to measure the electrode potential with respect to the reference electrode. The output of this differential amplifier was connected to the external signal input of the Autolab potentiostat. An earthed coaxial connector to both electrode leads was connected to the Autolab earth terminal.

## RESULTS AND DISCUSSION

The  $\text{Li}_2\text{Mn}_2\text{O}_4/\text{LiMn}_2\text{O}_4$  system in contact with a lithium ion electrolyte (3 phases, two components) has only one degree of freedom and therefore for a given lithium concentration there is a unique value of electrode potential. The response of the  $\text{Li}_2\text{Mn}_2\text{O}_4/\text{LiMn}_2\text{O}_4$  covered Au ring electrode in different aqueous LiCl solutions is shown in Figure 1.

FIGURE 1 HERE

A linear response of the ring potential vs. the  $\log [\text{Li}^+]$  has been observed with a slope 50-60 mV according to the reaction:



The potentiometric measurement at the ring electrode is based on a calibration curve:

$$E = E^0 + S \cdot \log [\text{Li}^+]_{surf} \quad (8)$$

with S close to -60 mV per ten fold  $\text{Li}^+$  concentration at low concentration and -40 mV slope at high concentration. Similar calibration curves were obtained in organic solvents containing lithium salts.

### a) Oxygen Reduction on Au in 80 mM $\text{LiPF}_6$ in DMSO

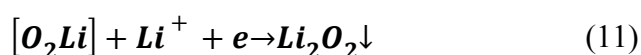
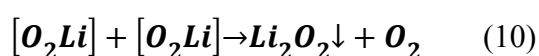
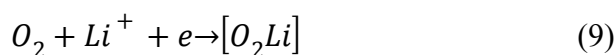
We first consider the measurement of lithium ion flux during the reduction of oxygen in dilute  $\text{LiPF}_6$  in DMSO electrolyte. Figure 2A shows the cyclic voltammetry of a rotating Au disc electrode with an Au ring coated with  $\text{Li}_2\text{Mn}_2\text{O}_4/\text{LiMn}_2\text{O}_4$  in 1 atm  $\text{O}_2$  saturated 80 mM  $\text{LiPF}_6$  in DMSO electrolyte at 9 Hz.

FIGURE 2 HERE

A characteristic feature of this reaction in lithium containing electrolyte is the cathodic current maximum which has been ascribed to the formation of a solid deposit of  $\text{Li}_2\text{O}_2$



blocking the electrode.[18] RRDE studies in amperometric mode have shown that DMSO stabilizes  $O_2^-$  ion in the first electron transfer step to oxygen.[16, 19, 20] The ring potential minimum,  $E_R$ , indicates that the flux of soluble  $Li^+$  ions increases the larger the ORR overpotential and then decreases due to surface passivation, due to either disproportionation or a two electron transfer to  $O_2$  from the electrode, according to the accepted mechanism:[21]



Two different mechanisms for the ORR in  $Li^+$ -containing non aqueous solvents have recently been proposed [21, 22], depending on the growth of  $Li_2O_2$  at the cathode surface: a surface reaction or a solution-phase reaction. In the surface mechanism, two adsorbed  $LiO_2$  molecules can disproportionate at the electrode surface or undergo two sequential one-electron transfer steps. It is worth noting that reactions (7) and (9) consume lithium ions while soluble superoxide can react with lithium ions, to further dismutate by reaction (10):

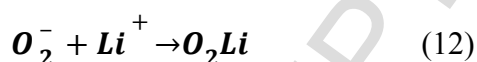


Figure 2 depicts the ring electrode potential,  $E_R$ , simultaneous to the ORR disc current,  $I_D$ , response.  $E_R$  measures the surface concentration of lithium ion  $[Li^+]_{surf}$  which can be calculated with eqn. (8) and (13):

$$\Delta E = E - E^* = s \log \frac{[Li^+]_{surf}}{[Li^+]^*} \quad (13)$$

A sharp drop of the lithium ion concentration can be observed at the onset of ORR close to 3 V, therefore there is convective-diffusion flux of lithium ions towards the Au disc electrode while  $O_2$  reduction takes place as expected from the previous mechanisms.

The potentiometric lithium ring electrode response is fast, i.e. with a rise time of less than 5 seconds, therefore the slow recovery of the  $E_R$  and thus the surface lithium ion concentration should be ascribed to slow processes at the disc electrode and not to the potentiometric ring response. Complete depletion of lithium ions at the surface occurs before the cathodic ORR maximum is attained, thus the flux of  $\text{Li}^+$  limits the rate of ORR and therefore the cathodic current at the disk.

An interesting feature in Fig. 2 is that while the Au disc is completely passivated and the current drops to zero, in the back sweep the lithium surface concentration recovers very slowly. Thus, a flux of lithium ions is still observed while there is no supply of electrons at the disk electrode. We interpret this result by soluble surface superoxide accumulated in the solution adjacent to the Au cathode and continue to react with lithium to deposit  $\text{Li}_2\text{O}_2$  according to reactions (10) and (8), which is consistent with our previous report on  $\text{LiO}_2$  dismutation.[6] This interesting result can be obtained with the unique capability of the potentiometric RRDE to assess the surface concentration of lithium ions.

#### b) Intercalation of lithium ions in $\text{LiMn}_2\text{O}_4$ in aqueous solutions

A second example of the RRDE potentiometric technique is the intercalation/de-intercalation of  $\text{Li}^+$  in the spinel  $\text{LiMn}_2\text{O}_4$  from aqueous  $\text{LiCl}$  solutions. Figure 3 depicts a typical cyclic voltammetry at low scan rate ( $2 \text{ mV}\cdot\text{s}^{-1}$ ) of  $\text{LiMn}_2\text{O}_4/\text{Au}$  disc electrode in contact with  $0.1 \text{ M LiCl}$  at  $9 \text{ Hz}$  and the simultaneous potentiometric response of the ring electrode,  $E_R$ .

It should be noticed that in this experiment a thin porous layer of  $\text{LiMn}_2\text{O}_4$  on the Au disc non flat surface presents problems to strictly apply the theory of the RDE as has been discussed elsewhere. [23-25]. However, we are not interested to extract electrode kinetics but to show how a lithium flux at the disc electrode can be followed by the potentiometric RRDE.

The current potential curve in Figure 3 exhibits two sets of anodic, A1 and A2, and two cathodic peaks, C1 and C2 in the potential range between 0.2 and 1.2 V as has been reported elsewhere [5, 6] which have been ascribed to a two-step delitiation-litiation insertion process between  $\text{LiMn}_2\text{O}_4$  and  $\lambda\text{-MnO}_2$ [26, 27]. These peaks correspond to the Li-ion insertion/extraction due to the simultaneous redox change in the  $\text{Mn}^{\text{III}}/\text{Mn}^{\text{IV}}$  in the spinel host structure. We have restricted the potential window in order to keep the lithium stoichiometry within the  $0 \leq x \leq 1$ .

In Figures 3 the intercalation-deintercalation of lithium ions in the  $\text{LiMn}_2\text{O}_4$  deposited at the disc electrode depends on the initial state of charge (SOC). Notice that the initial curve (start) is different to the following curve and that a steady state is approached. However, the potentiometric measurement shows that the surface lithium concentration evolves much slowly but follows the same trend.

FIGURE 3 HERE

It should be noticed that the potentiometric ring response follows the current-potential voltammetric curve. During oxidation of  $\text{Mn}^{\text{III}}$  and release of lithium ions in solution the increase of  $E_D$  is indicative of a larger surface  $\text{Li}^+$  concentration than in the bulk solution, and conversely during reduction of  $\text{Mn}^{\text{IV}}$  and insertion of lithium from the aqueous electrolyte a decrease of  $E_D$  is observed. Eqn. 6 shows that a difference in lithium ion concentration between the surface and bulk solution results form a net flux of  $\text{Li}^+$  ions at the  $\text{Li}_{1-x}\text{Mn}_2\text{O}_4$  / electrolyte interface. Notice that the potentiometric ring response to surface  $\text{Li}^+$  ions also detects the presence of the two ion exchange transitions in the  $\lambda\text{-MnO}_2/\text{Li}_{1-x}\text{Mn}_2\text{O}_4$  system within  $0 \leq x \leq 1$ . The transition between the two  $\text{Mn}^{\text{III}}/\text{Mn}^{\text{IV}}$  redox systems occurs at  $\text{Li}_{0.5}\text{Mn}_2\text{O}_4$  composition and corresponds to half-filled tetrahedral 8a sites in the spinel structure [9] available for lithium insertion into  $\lambda\text{-MnO}_2$ . There are

two sets of non-equivalent 8a sites which can be occupied in  $\text{Li}_x\text{Mn}_2\text{O}_4$  (with  $x \leq 1$ ) respectively by four lithium ions each leading to two peaks in the cyclic voltammetry.

A quantitative analysis can be done with repetitive oxidation-reduction current pulses as depicted in Figure 4.

FIGURE 4 HERE

While the  $\text{Li}_{1-x}\text{Mn}_2\text{O}_4/\text{Au}$  disc potential evolves as expected during  $\pm 20 \mu\text{A}$  ( $\pm 0.1 \text{ mA}\cdot\text{cm}^{-2}$ ) constant current pulses [5, 6], the potentiometric  $E_R$  response to surface lithium concentration follows similar symmetric pulses with respect to the unperturbed LMO system and returns to this rest potential value at zero disc current.

The variation  $\Delta[\text{Li}^+]$ , in the disc surface  $\text{Li}^+$  concentration can be calculated with eqn. (8). The bulk lithium ion analytical concentration is  $[\text{Li}^+]^* = 0.1 \text{ M}$ ; when we apply a constant current to the disc electrode a flux of lithium ions should result and thus the surface concentration  $[\text{Li}^+]_{\text{surf}}$  will be different from the bulk concentration and the ring electrode potential will detect the change.

For  $\pm 6 \text{ mV}$  shift in  $E_R$  as seen in Fig. 4, we calculate with eqn. (13),  $[\text{Li}^+] = 0.126 \text{ M}$  and  $0.079 \text{ M}$  respectively for the oxidation and the reduction currents. The concentration gradient is then,

$$\Delta[\text{Li}^+] = [\text{Li}^+]_{\text{surf}} - [\text{Li}^+]_{\text{bulk}} \quad (14)$$

and results  $0.026$  and  $-0.021 \text{ M}$  respectively.

While the  $\text{Li}_{1-x}\text{Mn}_2\text{O}_4/\text{Au}$  disc potential evolves as expected during  $\pm 20 \mu\text{A}$  ( $\pm 0.1 \text{ mA}\cdot\text{cm}^{-2}$ ) constant current pulses [5, 6], the potentiometric  $E_R$  response to surface lithium concentration follows similar symmetric pulses with respect to the unperturbed LMO system and returns to this rest potential value at zero disc current.

The variation  $\Delta[Li^+]$ , in the disc surface  $Li^+$  concentration can be calculated with (8). The bulk lithium ion analytical concentration is  $[Li^+]^* = 0.1$  M; when we apply a constant current to the disc electrode a flux of lithium ions should result and thus the surface concentration  $[Li^+]_{surf}$  will be different from the bulk concentration and the ring electrode potential will detect the change.

An interesting new evidence has been obtained with the potentiometric RRDE measurement of lithium ion fluxes during insertion-deintercalation of lithium ions at the  $LiMn_2O_4$ /aqueous lithium electrolyte interface at extreme anodic and cathodic potentials. During a deep oxidation (de-litiation) at a constant current  $200 \mu A$  the disc electrode potential exceeds  $1.1$  V and the potentiometric ring electrode potential exhibits a fast growth above the constant value expected for the applied current which indicates that the  $Li^+$  ion surface concentration increases dramatically over the flux imposed by the applied constant current (Figure 5). The dashed line indicates the end of the current step and the open circuit decay of  $E_R$  shows the slow equilibration of the solid oxide with the liquid lithium ion electrolyte.

The flux of lithium ions larger than expected for a constant  $200 \mu A$  constant current results from a massive decomposition of the electrode material as verified by oxygen evolution measured by differential electrochemical mass spectrometry (DEMS) experiments under similar conditions.[28]

FIGURE 5 HERE

Conversely, during reduction of  $Li_xMn_2O_4$ , the potential drops below  $0.2$  V and an abrupt decrease of  $E_R$  takes place which is indicative of a massive lithium flux probably due to dismutation of Mn(III) into Mn(IV) and soluble Mn(III) with release of lithium from the oxide (Figure 6).

In Figures 5 and 6 we observe at low charge a constant ring electrode potential and an evolution of the disc electrode potential during intercalation and de-intercalation of  $\text{Li}^+$  ions within the stability of  $\text{Li}_{1-x}\text{Mn}_2\text{O}_4$  ( $0 \leq x \leq 1$ ). Therefore, the flux of  $\text{Li}^+$  ions in the electrolyte exactly matches the flux of electrons in the solid oxide. However, when the LMO electrode potential exceeds above 1.2 V or below 0.4 V at the same constant current  $\pm 200 \mu\text{A}$ , potential runaway in the positive and negative directions and  $E_R$  shows that the flux of lithium ions in both anodic and cathodic processes exceeds the flux of electrons at constant current.

FIGURE 6 HERE

We speculate that at extreme potentials the LMO is massively de-lithiated upon oxidation, and massively lithiated during reduction. It is well known that Jahn-Teller effect results in phase transition of  $\text{LiMn}_2\text{O}_4$  to  $\text{Li}_2\text{Mn}_2\text{O}_4$  with dismutation of  $\text{Mn}^{\text{III}}$  into  $\text{Mn}^{\text{IV}}$  and soluble  $\text{Mn}^{\text{II}}$ .

At open circuit the ring potential evolves towards a decrease in surface lithium concentration as shown by the simultaneous ring potential drop towards the initial values as the  $\text{Li}^+$  ion fluxes drop to zero.

## CONCLUSIONS

We have demonstrated the potentiometric measurement of lithium ion fluxes using a  $\text{LiMn}_2\text{O}_4/\text{Li}_2\text{Mn}_2\text{O}_4$  electrode reversible to lithium ions, both in non aqueous solution during  $\text{O}_2$  reduction reaction and in aqueous solution during intercalation-deintercalation of  $\text{Li}^+$  in the spinel oxide.

While the flux of lithium matches the flux of electrons and molecular oxygen, at extreme potentials anodic and cathodic instability of the Li-Mn spinel oxide yields flux of lithium ions which is larger than the applied current due to oxide massive decomposition.

**ACKNOWLEDGEMENTS**

FS-Nano 07 and research postdoctoral and doctoral fellowships Funding from CONICET and ANPCyT PICT 2012

No. 1452 and from ANPCyT (M. del P)-

ACCEPTED MANUSCRIPT

## REFERENCES

- [1] W.J. Albery, E.J. Calvo, Ring-disc electrodes. Part 21. - pH measurement with the ring, *Journal of the Chemical Society, Faraday Transactions 1: Physical Chemistry in Condensed Phases*, 79 (1983) 2583-2596.
- [2] W.J. Albery, A.R. Mount, Ring-disc electrodes. Part 22. - Theory of the measurement of proton fluxes at the disc, *Journal of the Chemical Society, Faraday Transactions 1: Physical Chemistry in Condensed Phases*, 85 (1989) 1181-1188.
- [3] W.J. Albery, A.R. Mount, Ring-disc electrodes. Part 23. - Studies of proton fluxes at a thionine-coated electrode, *Journal of the Chemical Society, Faraday Transactions 1: Physical Chemistry in Condensed Phases*, 85 (1989) 1189-1198.
- [4] W.J. Albery, A.R. Mount, Ring-disc electrodes. Part 24. - Studies of counterion fluxes at a thionine-coated electrode, *Journal of the Chemical Society, Faraday Transactions 1: Physical Chemistry in Condensed Phases*, 85 (1989) 3717-3724.
- [5] L.L. Missoni, F. Marchini, M. Del Pozo, E.J. Calvo, A LiMn<sub>2</sub>O<sub>4</sub>-Polypyrrole battery system for the extraction of LiCl from natural brine, *J. Electrochemical Society*, 163 (2016) A1898-A1902.
- [6] F. Marchini, D. Rubi, M. Del Pozo, F.J. Williams, E.J. Calvo, Surface Chemistry and Lithium-Ion Exchange in LiMn<sub>2</sub>O<sub>4</sub> for the Electrochemical Selective Extraction of LiCl from Natural Salt Lake Brines, *Journal of physical Chemistry c*, 31 (33) (2016) 9236–9245.
- [7] D. Guyomard, J.M. Tarascon, Rechargeable Li<sub>1+x</sub>Mn<sub>2</sub>O<sub>4</sub>carbon cells with a new electrolyte composition, *Journal of the Electrochemical Society*, 140 (1993) 3071-3081.



- [8] J.M. Tarascon, D. Guyomard, Li metal-free rechargeable batteries based on  $\text{Li}_{1+x}\text{Mn}_2\text{O}_4$  cathodes ( $0 \leq x \leq 1$ ) and carbon anodes, *Journal of the Electrochemical Society*, 138 (1991) 2864-2868.
- [9] M. Rossouw, A. de Kock, L. de Picciotto, M. Thackeray, W. David, R. Ibberson, Structural aspects of lithium-manganese-oxide electrodes for rechargeable lithium batteries, *Materials Research Bulletin*, 25 (1990) 173-182.
- [10] H. Kanoh, K. Ooi, Y. Miyai, S. Katoh, Selective electroinsertion of lithium ions into a  $\text{Pt}/\lambda\text{-MnO}_2$  electrode in the aqueous phase, *Langmuir*, 7 (1991) 1841-1842.
- [11] K. Ooi, Y. Miyai, S. Katoh, H. Maeda, M. Abe, Topotactic  $\text{Li}^+$  insertion to  $\lambda\text{-MnO}_2$  in the aqueous phase, *Langmuir*, 5 (1989) 150-157.
- [12] Z.J. Barton, J. Rodríguez-López, Lithium ion quantification using mercury amalgams as in situ electrochemical probes in nonaqueous media, *Analytical Chemistry*, 86 (2014) 10660-10667.
- [13] Z.J. Barton, J. Rodríguez-López, Cyclic Voltammetry Probe Approach Curves with Alkali Amalgams at Mercury Sphere-Cap Scanning Electrochemical Microscopy Probes, *Analytical Chemistry*, 89 (2017) 2708-2715.
- [14] J.K. Novev, S. Eloul, R.G. Compton, Influence of Reaction-Induced Thermal Convection on the Electrical Currents Measured in Chronoamperometry and Cyclic Voltammetry, *Journal of Physical Chemistry C*, 120 (2016) 13549-13562.
- [15] W.J. Albery, Ring-disc electrodes: Part 1. - A new approach to the theory, *Transactions of the Faraday Society*, 62 (1966) 1915-1919.
- [16] W. Torres, N. Mozhzhukhina, A.Y. Tesio, E.J. Calvo, A rotating ring disk electrode study of the oxygen reduction reaction in lithium containing dimethyl sulfoxide electrolyte: Role of superoxide, *Journal of the Electrochemical Society*, 161 (2014) A2204-A2209.

- [17] A.W. Lodge, M.J. Lacey, M. Fitt, N. Garcia-Araez, J.R. Owen, Critical appraisal on the role of catalysts for the oxygen reduction reaction in lithium-oxygen batteries, *Electrochimica Acta*, 140 (2014) 168-173.
- [18] C.O. Laoire, S. Mukerjee, K.M. Abraham, E.J. Plichta, M.A. Hendrickson, Influence of nonaqueous solvents on the electrochemistry of oxygen in the rechargeable lithium-air battery, *Journal of Physical Chemistry C*, 114 (2010) 9178-9186.
- [19] M.J. Trahan, S. Mukerjee, E.J. Plicht, M.A. Hendrickson, K.M. Abraham, Studies of li-air cells utilizing dimethyl sulfoxide-based electrolyte, *Journal of the Electrochemical Society*, 160 (2013).
- [20] W.R. Torres, A.Y. Tesio, E.J. Calvo, Solvent co-deposition during oxygen reduction on Au in DMSO LiPF<sub>6</sub>, *Electrochemistry Communications*, 49 (2014) 38-41.
- [21] Z. Peng, S.A. Freunberger, L.J. Hardwick, Y. Chen, V. Giordani, F. Bardé, P. Novák, D. Graham, J.M. Tarascon, P.G. Bruce, Oxygen reactions in a non-aqueous Li<sup>+</sup> electrolyte, *Angewandte Chemie - International Edition*, 50 (2011) 6351-6355.
- [22] B.D. McCloskey, D.S. Bethune, R.M. Shelby, G. Girishkumar, A.C. Luntz, Solvents critical role in nonaqueous Lithium-Oxygen battery electrochemistry, *Journal of Physical Chemistry Letters*, 2 (2011) 1161-1166.
- [23] J. Masa, C. Batchelor-McAuley, W. Schuhmann, R.G. Compton, Koutecky-Levich analysis applied to nanoparticle modified rotating disk electrodes: Electrocatalysis or misinterpretation, *Nano Research*, 7 (2014) 71-78.

- [24] K. Ke, K. Hiroshima, Y. Kamitaka, T. Hatanaka, Y. Morimoto, An accurate evaluation for the activity of nano-sized electrocatalysts by a thin-film rotating disk electrode: Oxygen reduction on Pt/C, *Electrochimica Acta*, 72 (2012) 120-128.
- [25] S. Treimer, A. Tang, D.C. Johnson, A consideration of the application of Koutecký-Levich plots in the diagnoses of charge-transfer mechanisms at rotated disk electrodes, *Electroanalysis*, 14 (2002) 165-171.
- [26] A. Rougier, K.A. Striebel, S.J. Wen, E.J. Cairns, Cyclic voltammetry of pulsed laser deposited  $\text{Li}_x\text{Mn}_2\text{O}_4$  thin films, *Journal of the Electrochemical Society*, 145 (1998) 2975-2980.
- [27] D. Guyomard, J.M. Tarascon, Rocking-chair or lithium-ion rechargeable lithium batteries, *Advanced Materials*, 6 (1994) 408-412.
- [28] F. Marchini, LiCl electrochemical recovery from argentine natural brines using  $\text{LiMn}_2\text{O}_4$  electrodes, DQIAyQF. Facultad de Ciencias Exactas y Naturales, Universidad de Buenos Aires, Buenos Aires, Argentina, 2018, pp. 216.

**FIGURE CAPTIONS****Figure 1.**

Potentiometric calibration curve with a  $\text{Li}_2\text{Mn}_2\text{O}_4/\text{LiMn}_2\text{O}_4$  Au ring electrode for  $i_D = 0$  in LiCl aqueous solution vs. Ag/AgCl; 3M KCl.

## Figure 2:

$\text{O}_2$  reduction polarization curve on an Au disc electrode in 1 atm  $\text{O}_2$  saturated 80 mM  $\text{LiPF}_6$  in anhydrous DMSO at  $W = 9$  Hz and simultaneous potentiometric ring potential,  $E_R$ , Sweep rate  $0.1 \text{ V}\cdot\text{s}^{-1}$ . Reference electrode:  $\text{LiMn}_2\text{O}_4/\text{Li}_2\text{Mn}_2\text{O}_4$  in 1 M  $\text{LiPF}_6$  in DMSO.

## Figure 3.

Cyclic voltammetry of  $\text{LiMn}_2\text{O}_4/\text{Au}$  disc electrode of RRDE in 0.1 M  $\text{LiNO}_3$  aqueous solution at 9 Hz,  $2 \text{ mV}\cdot\text{s}^{-1}$  (lower panel) and simultaneous potentiometric ring response  $E_R$  (vs. Ag/AgCl; 3M KCl) to lithium ion concentration on the surface (upper panel). Reference electrode: Ag/AgCl; 3M KCl

## Figure 4:

Disk and ring potential response to  $\pm 20 \mu\text{A}$ . current pulses at the  $\text{Li}_x\text{Mn}_2\text{O}_4/\text{Au}$  disc electrode of a RRDE at 9 Hz in 0.1 M aqueous LiCl. Reference electrode: Ag/AgCl; 3M KCl.

## Figure 5:

$\text{LiMn}_2\text{O}_4$  disk potential and  $E_R$  responses to a  $200 \mu\text{A}$  anodic current pulse and relaxation at open circuit potential in 0.1 M aqueous  $\text{LiNO}_3$  solution. Reference Electrode: Ag/AgCl; 3M KCl

Figure 6.  $\text{LiMn}_2\text{O}_4$  disk potential and  $E_R$  responses to a  $-200 \mu\text{A}$  cathodic current pulse and relaxation at open circuit potential in 0.1 M aqueous  $\text{LiNO}_3$  solution. Reference Electrode: Ag/AgCl; 3M KCl.

Figure 1

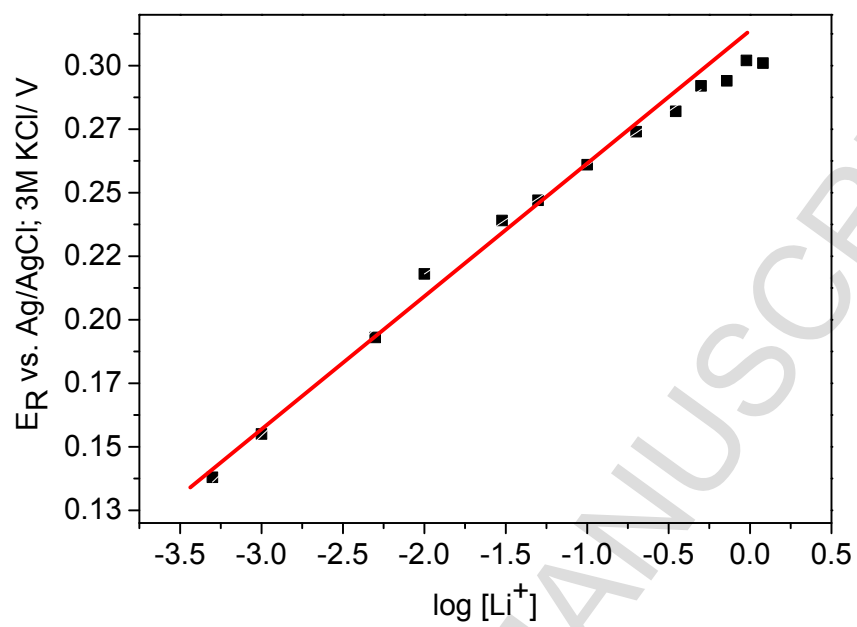


Figure 2

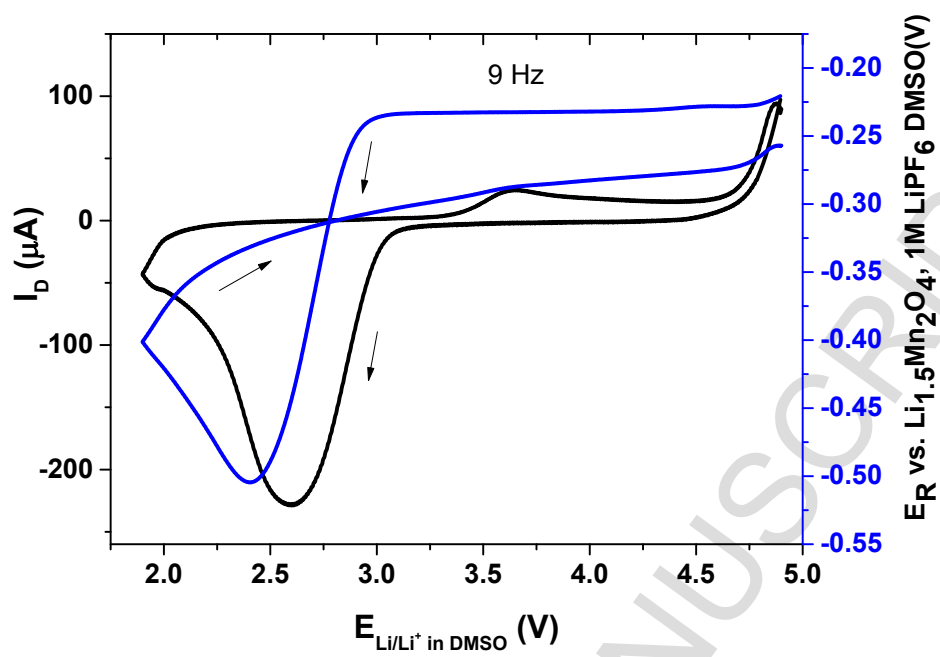


Figure 3

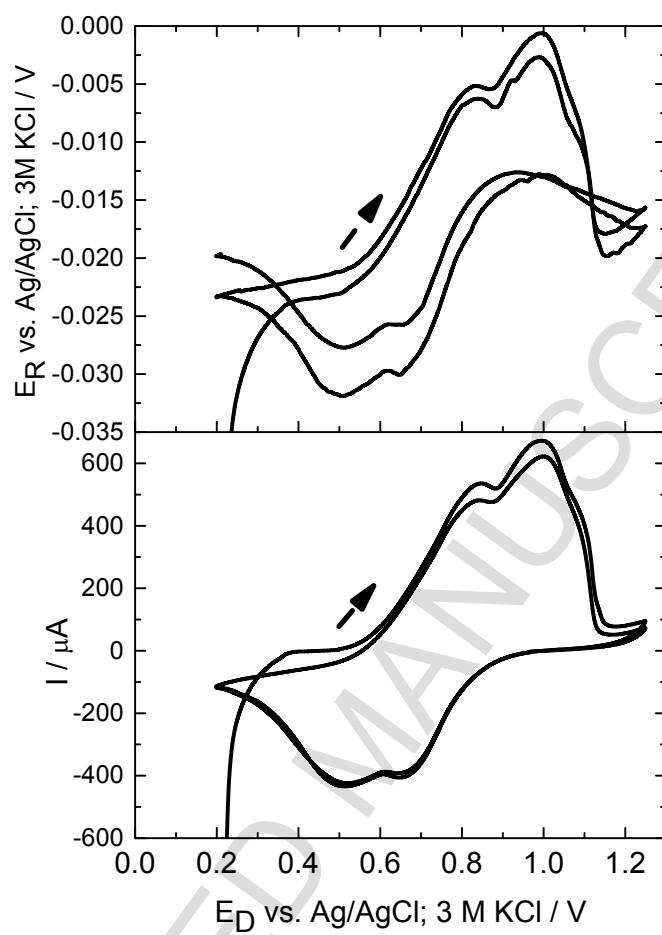


Figure 4

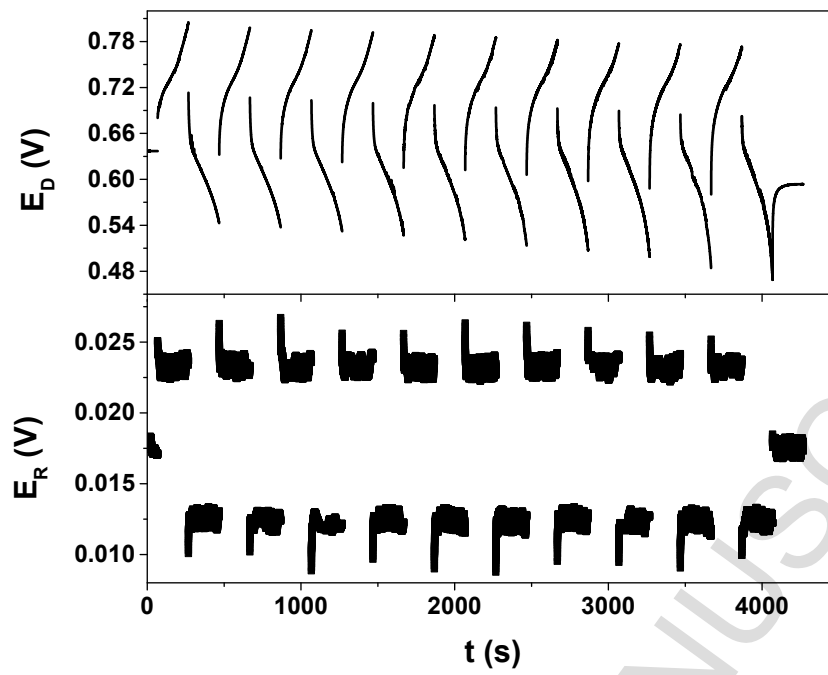




Figure 5

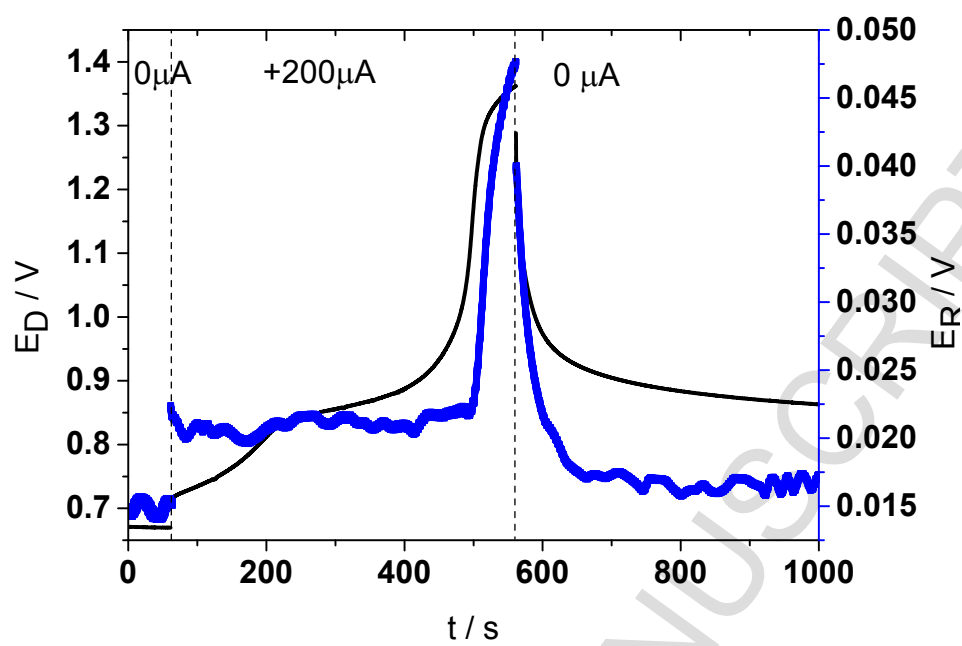
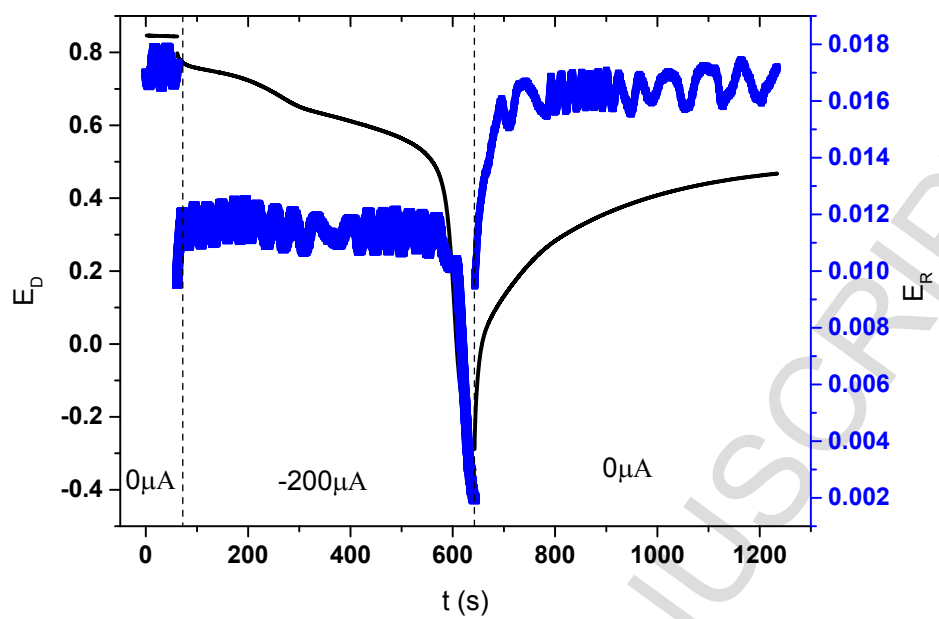
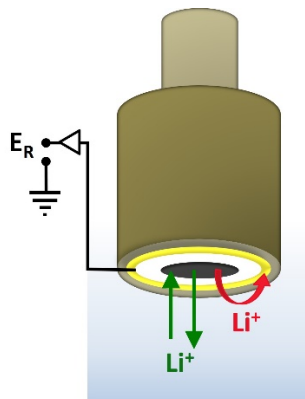


Figure 6



## Graphical Abstract

Potentiometric detection of lithium ions with a rotating ring disc electrode (RRDE), allow direct measurement lithium ion fluxes simultaneously to electron fluxes.



ACCEPTED MANUSCRIPT

ACCEPTED MANUSCRIPT